RAMAN CRYSTALLINITY AND HALL EFFECT STUDIES OF MICROCRYSTALLINE SILICON SEED LAYERS

T. N. Nyang'onda[1], D. M. Mulati[2] and B. O. Aduda[3]
[1,3]University of Nairobi, Nairobi, Kenya
[2] Jomo Kenyatta University of Agriculture and Technology, Nairobi, Kenya
Email: nyangondat@uonbi.ac.ke

Abstract

Aluminium induced crystallization (AIC) was used to crystallize sputtered amorphous silicon thin films on aluminium-coated glass at annealing temperatures ranging from 250-520°C in vacuum. Crystalline volume fractions were measured by Raman spectrometry as a function of annealing temperature. It was shown that the crystallized films had large grains as the Raman peaks were centred at about 520 cm^{-1} at and over annealing temperatures of 420°C. The three-layer sample crystallization resulted in crystallization of the films at lower temperatures compared to the two-layer sample crystallizations which implied a reduction in the cost of production of the seedlayer and resulting products. Hall mobilities and hole densities ranging from 17.0-22.8 $cm^2V^{-1}s^{-1}$and (4.7-9.2) × 10^{18} cm^{-3} respectively were measured. Low hole charge densities for films of the same thickness were achieved at high annealing temperatures which was an indication of less aluminium in seed layers prepared at those temperatures. Having seed layers with sufficiently low hole charge densities is desirable for application of the seed layer in photovoltaic applications.

Key Words: microcrystalline, silicon, annealed, raman, crystallinity, hall-effect

1.0 Introduction

Progress in the attainment of high efficiencies of microcrystalline silicon (μc-Si) solar cells may require the use of μc-Si seed layers grown by metal induced crystallization (MIC). Metal induced crystallization typically takes from a few minutes to 3 hours unlike in solid phase crystallization usually done at about 600 °C that takes about 24 hours (Nast and Hartmann, 2000; Pelant *et al.*,2002). Aluminium induced crystallization (AIC) of amorphous silicon is a layer exchange process whereby upon etching of aluminium, a mixture of aluminium and silicon remains on top of the underlying microcrystalline silicon. The Al+Si is removed by wet chemical etching and the rough surface that results is smoothened by chemical mechanical polishing (CMP) (Gall, 2007). The growth of optimal large grains by MIC of these seed layers reduces the effect of recombination at the grain boundaries. Microcrystalline silicon is normally grown by plasma enhanced chemical vapour deposition (PECVD) (Gordijin *et al*., 2006; Kondo *et al*., 2003) and by hot wire chemical vapour deposition (HWCVD) (Mahan, 2003) due to high deposition rates obtained by use of these methods and the yield of device quality materials. However silane gas used in these processes is inflammable, the equipment for PECVD is expensive and the grain sizes are generally small. A number of researchers have worked on the crystallization of amorphous silicon (a-Si) on aluminium-coated glass (Nast *et al*., 1998; Schneider *et al*., 2006; Lee *et al*., 2007) or of thin layer of aluminium on a-Si coated glass (Wang *et al*., 2008), but a handful of papers on the crystallization of a-Si sandwiched between the aluminium (Chandan *et al*., 2006). Other workers have done crystallization of a-Si using AIC on wafer substrates (Ishikawa *et al*., 2004)

Efficiencies of thin-film silicon solar cells have been found to generally increase with grain size (Dimova-Malinovska, 2005). Yamamoto (2003) showed that the open circuit voltage (V_{oc}) generally increased with grain size. The difference in grain size is due to different preparation methods. Jaeger *et al*. (2008) prepared thin (20 nm) microcrystalline silicon seed layers by aluminium induced crystallization by annealing at 550 °C. These seed layers had a mobility of 21 $cm^2V^{-1}s^{-1}$, a hole density and conductivity in the order of 10^{19} cm^{-3} and 10^1 S cm^{-1} respectively. Passivation of the films varied the conductivity exponentially from 10^{-4} to 10^{-9} S cm^{-1} and dark conductivity activation energy from 14 meV to 202 meV in the 5-300 K temperature range. Hyeongnam *et al*. (2002) obtained Hall hole concentrations, mobility and resistivities of (3.8 - 7.0) × 10^{18} cm^{-3}, 19.9 - 36.5 $cm^2V^{-1}s^{-1}$ and 0.037 - 0.045 Ω cm respectively for aluminium induced crystallized layers on glass annealed at 500 °C. High mobilities of 80 $cm^2V^{-1}s^{-1}$ of polycrystalline silicon films prepared by thickening aluminium induced crystallization seed layers on wafer substrates using atmospheric pressure chemical vapour deposition have been obtained (Ishikawa, 2004). The thermodynamics and mechanism of MIC, origin of MIC and tailoring of the crystallization temperature of a-Si by using ultra thin aluminium layers has been explained by Wang *et al*. (Wang *et al.,* 2006, 2008a, 2008b) respectively. *In-situ* AIC has so far been done by a few people (Hong and Ro, 2007; Gupta *et al., 2008;* Wang

et al., 2009). In one of those studies using Joule induced in situ crystallization at temperatures of 600-1000 °C, a high temperature glass has to be used which is expensive compared to the normal glass. Furthermore, attempt was not made to measure the hole charge densities in order to ascertain whether the films can be used for photovoltaic applications. AIC seed layers usually have high charge densities (10^{18}-10^{20} cm^{-3}) and high electrical conductivities in the order of 10^{1}-10^{2} S cm^{-1} (Jaeger *et al., 2008*). One of the uses of microcrystalline silicon from AIC is to use it as a seed layer in photovoltaic applications.

This study therefore focuses on Raman crystalline volume fractions and Hall measurements of crystallized two-layer and three-layer structures in order to ascertain the benefits of each of the two types of crystallizations. The issue of the onset of crystallization for the two structures will be compared. Raman analysis and Hall effect of microcrystalline silicon thin films grown by AIC of sputtered a-Si were done in order to explore their use as seed layers in Glass/ZnO:Al/p^{+}*pin*/ZnO:Al µc-Si solar cells.

2.0 Materials and Methods

Amorphous silicon and aluminium thin films were prepared using *Edwards 306* coating unit of 13.56 MHz frequency. The argon flow rate from the cylinder in both cases was 22 $cm^{-3}s^{-1}$. Aluminium was prepared by DC magnetron sputtering at a process pressure of 4×10^{-3} mbar while silicon films were deposited at 2×10^{-3} mbar using RF sputtering and the sputtering power in both cases was 400 W. The thickness ratio of Al : a-Si was 1:2 for the two-layer samples (Glass/Al/a-Si) while that for Al: a-Si: Al was 1:2:1 for the three-layer samples (Glass/Al/a-Si/Al) (other ratios were not investigated). Deposition rates for aluminium and amorphous silicon were 0.30 nm/s and 0.11 nm/s respectively. Undoped multicrystalline silicon target of 7.620 cm diameter by 0.625 cm thickness and aluminium target of the same dimensions were used and both had purity of 99.999 %. Samples were not intentionally heated and the vertical distance between the substrate and the targets was about 30.5 cm. Rotation of the samples was done for uniform deposition of the films. Samples were initially annealed for one hour at 520 °C in vacuum as trial run and later for three hours at temperatures ranging between 250 - 520 °C in vacuum. The heating rate to the annealing temperature was 17 °C/min and after annealing, the heater power supply was disconnected and the samples were left to cool to room temperature in vacuum.

Etching of aluminium was done using concentrated mixtures of 80% phosphorous acid, 5% acetic acid, 5% nitric acid and 10% of de-ionized water at 50 – 55 °C (Nast *et al., 1998*). Raman crystalline volume fraction analysis was then done using a red wavelength light. The distribution of the particles was analyzed using scanning probe image processor (SPIP) sofware using the simple threshold detection method. Threshold type was set to fixed level and particle threshold level was set to 218.86

nm while post processing parameters were: Preservation of holes in shapes, non smoothening of the shape contours and inclusion of the shapes on border. A minimum area filtering of 0.5 μm^2 was used. Regions of large and small crystallites were observed using a Nikon L 200 optical microscope. Raman data was then collected on parts of the sample with large grains. Hall-effect measurements were done using the standard Van der Pauw method (*Keithley 926* Hall profiler) which consisted of making four contacts with silver paste on the samples from which two of them were used for current and the other two for Hall voltage measurements. The Hall profiler was interfaced with a computer and the measurements were recorded automatically. In order to obtain comparable Hall results, we used films of the same thickness (0.4±0.1) μm. During the process of taking Hall measurements, it was found desirable to increase the current through the sample due to the high resistance of the films in order to take measurements.

3.0 Results and Discussions

3.1 Raman Crystalline Volume Fractions

Figure 1 below shows the normalized crystalline volume fractions as measured by Raman spectroscopy for samples annealed at 520 °C for one hour with spectra for amorphous silicon (a-Si) and monocrystalline silicon (c-Si) references also shown.

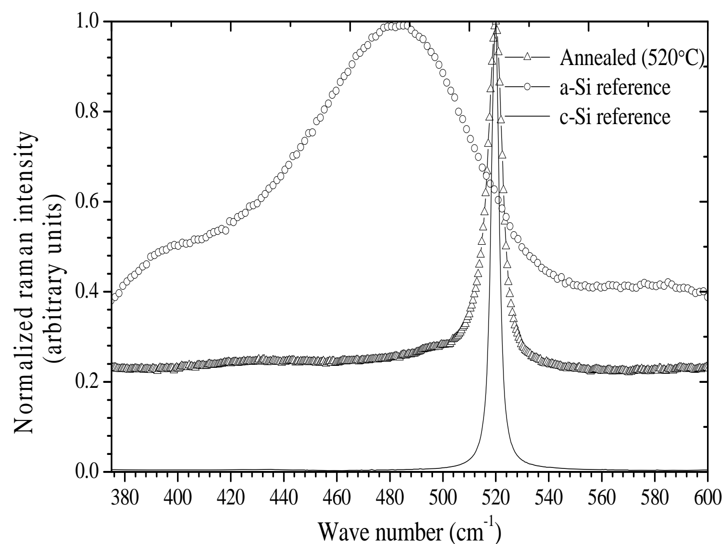

Figure 1: Normalized Raman intensity versus wave number of :
(1) Samples (glass/Al/a-Si) annealed at 520 °C for one hour
(2) a-Si reference (3) Monocrystalline silicon reference

The spectrum of the a-Si reference has a broad peak centred at about 480 cm^{-1}. The Raman spectra of samples of the glass/Al/a-Si series that were annealed for one hour had peaks centred at 520 cm^{-1} and their crystalline volume fraction was 85%. The spectra however contains a-Si component as it was not subtracted in the crystalline volume fraction calculations. Figure 2 shows the normalized Raman

spectra for a sample annealed for three hours at 520 °C (88% crystalline fraction) when amorphous silicon is not subtracted and when a-Si component is subtracted (crystalline part). Here we see a Raman peak centred at 520 cm^{-1} as in monocrystalline silicon. Annealing the layers for more time increased the crystalline volume fractions as expected. The corrected normalized Raman crystalline volume fraction of µc-Si films from annealed glass/Al/a-Si as a function of annealing temperature is shown in figure 3. Increasing the annealing temperature shifts the centre of the peaks towards the 520 cm^{-1} wave number (inset graph) which is the peak value for monocrystalline silicon. Centralization of the peak at 520 cm^{-1} is an indication that the material is largely polycrystalline, i.e., has less microcrystalline phase.

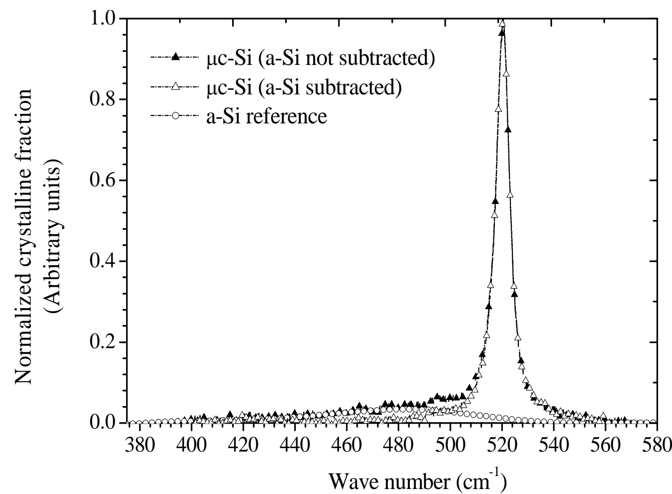

Figure 2: Normalized Raman crystalline fractions of polycrystalline silicon from annealed glass/Al/a-Si at 520 °C for three hours in vacuum and spectrum for a-Si reference

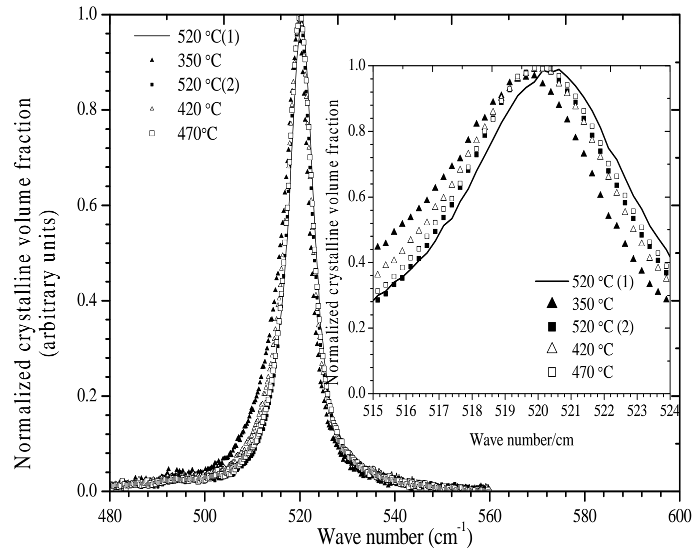

Figure 3: Raman crystalline volume fractions of microcrystalline silicon films from annnealed glass/Al/a-Si annealed for 3 hours in vacuum . The peak centres shifts towards 520 cm^{-1} as the annealing temperature increases (inset graph).

Results for two samples annealed at 520 °C are also shown in order to test for the reproducibility of the results. The difference in the results indicated that the crystallization was not homogenous; that is microcrystalline silicon is a mixture of large and small grains. In figure 4, we see that the full width at half maximum (FWHM) is inversely proportional to the annealing temperature due to the increase in crystallinity of the samples with annealing temperature.

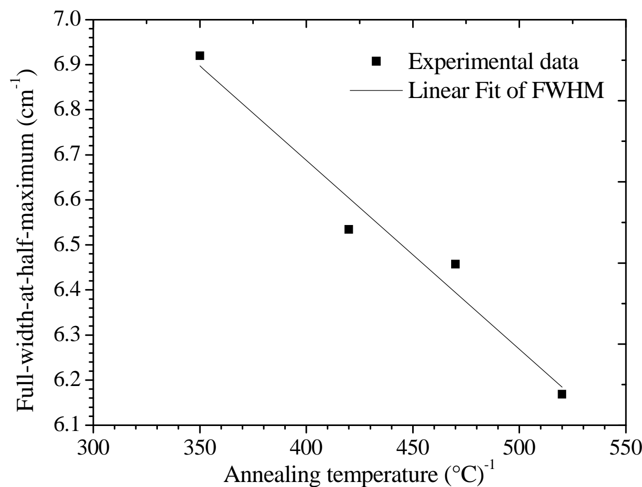

Figure 4: Full-width-at-half-maximum (FWHM) of the Raman crystalline volume fraction peaks with annealing temperature of microcrystalline silicon from annealed glass/Al/a-Si layers.

Crystalline volume fractions against crystallization temperature of annealed glass/Al/a-Si and glass/Al/a-Si/Al layers are shown in figure 5.

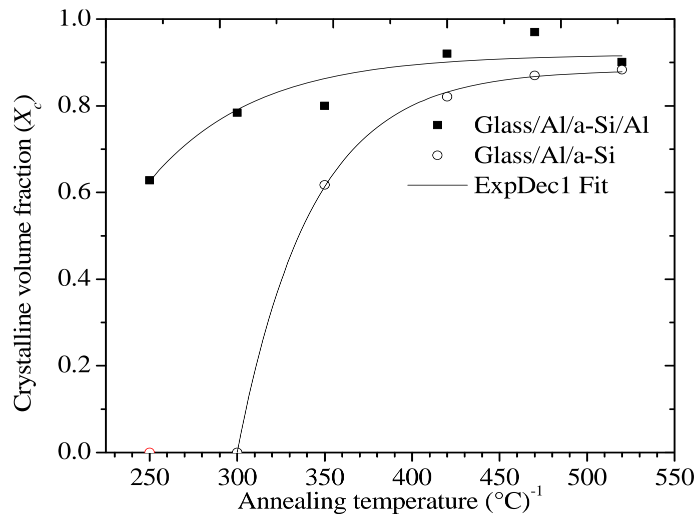

Figure 5: Raman crystalline volume fractions of μc-Si films after three hour anneal of Glass/Al/a-Si and Glass/Al/a-Si/Al layers for three hours in vacuum

The onset of crystallization (X-axis intercept) of the glass/Al/a-Si layers was 300 °C while for the glass/Al/a-Si/Al it was 180 °C (Figure 6). This latter temperature is within the 150-200 °C minimum temperature range obtained by (Wang *et al., 2006*). Crystallization temperatures of 165 °C have been reported (He *et al., 2005*). The seed layers with a aluminium doped zinc oxide can be used in solar cells in the Glass/ZnO:Al/p^{+}*pin/*TCO configuration. Sheet resistance of ZnO:Al/polysilicon (≈ 4 Ω/□) on glass substrate have been found to be very stable at annealing temperatures ranging between 425-600 °C at annealing times ranging between four to twenty hours (Lee *et al., 2007*).

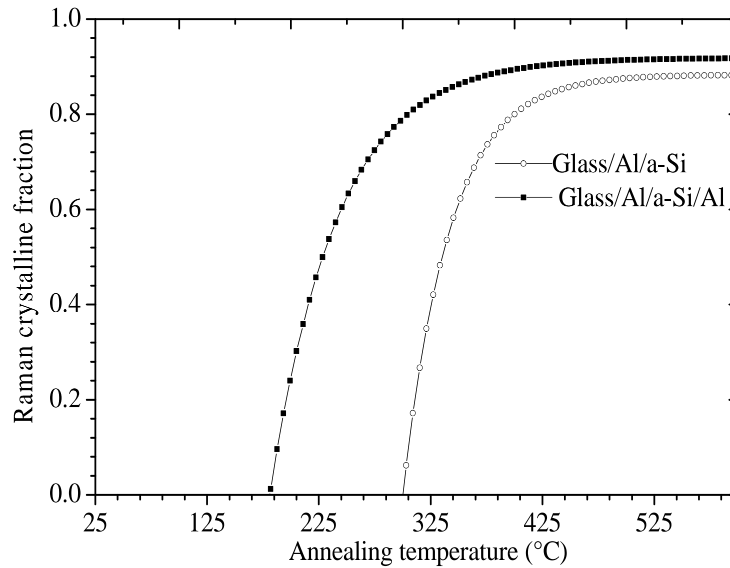

Figure 6: Fitting function plots of Raman crystalline fractions of microcrystalline silicon from three hour anneal of Glass/Al/a-Si and Glass/Al/a-Si/Al layers in vacuum

The equations of the fitted curves in figure 6 for microcrystalline silicon from annealed glass/Al/a-Si and glass/Al/a-Si/Al layers are given by equations (1) and (2) respectively.

$$X_c(T_A) = 0.88 - 1073\exp(-T_A/42) \quad (1)$$

$$X_c(T_A) = 0.92 - 18\exp(-T_A/60) \quad (2)$$

Where $X_c(T_A)$ is the crystalline volume fraction as a function of annealing temperature (T_A). These equations are in the form:

$$X_c(T_A) = A - B\exp(-KT_A) \quad (3)$$

Where $A \approx 1$ and *B* and *K* are greater than zero. Equations (3) becomes similar to the Avrami equation (Rojas-Lopez *et al., 2007*), when B=1, and $T_A = t^n$, the equation is given as:

$$X_c(t) = 1 - \exp(-Kt^n) \quad (4)$$

where $X_C(t)$ is the Raman crystalline volume fraction as a function of time, since equations (3) and (4) can be written as:

$X_c(T_A) = f(T_A)$ and $X_c(T_A) = f(t)$

and both functions are exponential functions with the exponential part of the equations giving the fraction of the material which is not yet crystallized.

In the Avrami equation, *K* is rate parameter and is temperature dependent, t is the crystallization time and *n* is an adjustable parameter that depends on the statistical model used (it was initially taken as an integer between 1 and 4 according to the original model). Our equations are for crystalline volume fractions as a function of annealing temperature. The nature of the crystals formed is described in (Avrami, 1939) as follows: In the case of isothermal crystallization which are usually "S" shaped curves, the ratio of the time for 75% transformation (crystallization) of the material to the time for 25% transformation of the material (t_{75}/t_{25}) can describe the type of growth. Ratios of between 1.48 and 1.69, 1.69 and 2.2 and between 2.2 and 4.82 are characteristic of polyhedral, plate-like and lineal (needle-like) growths (flatter curves) respectively;a less steep curve as for glass/Al/a-Si/Al layers in figure 6 indicates the formation of needle-like crystals at low crystallization temperatures.

3.2 Grain Size Distributions

Figure 7 shows particle area distributions of samples annealed at 470 and 520 °C in vacuum. Samples annealed at 520 °C had a large number of small particles less than 1 μm^2 compared with samples annealed at 470 °C. The grain sizes of samples prepared at 470 °C were generally larger compared to those for samples prepared at 520 °C for particles sizes of area greater than 20 μm^2.

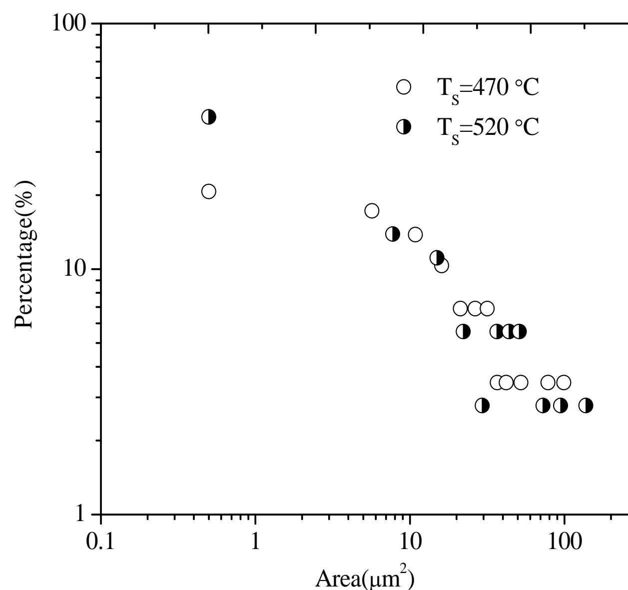

Figure 7: Particle area distribution of samples annealed

Microcrystalline silicon by AIC has a mixture of large and small grains. The large grains become dominant as the annealing time and temperature increases and

eventually the whole film becomes completely microcrystalline. However, comparision of Raman signal from large and small grains was not investigated in this work. The seed layer surface has to be chemically smoothened or polished before epitaxial growth is done.

3.3 Hall Effect

Mobility measurements in the Table 1 below indicate that as the annealing temperature increases, the carrier concentration decreases probably due to completion of the aluminium layer exchange process. Samples of same thicknesses annealed at 520 °C for three hours had a low charge concentration of 4.7×1018 cm-3 compared to 5.4×1018 cm-3for those annealed at the same temperature for one hour. This reduction in charge density is thought to be due to an increase in the aluminium segregation process with increase in annealing time. These hole densities were lower than those measured at annealing temperature of 470 °C (9.2×1018 cm-3). The results in the table also suggest an inverse relationship between hole density and resistivity as expected. Our resistivities were in the order of 10-2 Ωcm. Low charge denstity is an indication of less aluminium in sample hence high resistivity. Hole mobilities of 17.3 and 17.9 cm2 V-1s-1 were measured for samples annealed at 470 °C and 520 °C for three hours respectively and mobility of 22.8 cm2 V-1s-1 for a sample annealed at 520 °C for one hour. Hyeongnam et al. [20] obtained Hall hole concentrations, mobility and resistivities of (3.8 - 7.0) × 1018 cm-3, 19.9 - 36.5 cm2V-1s-1 and 0.037 - 0.045 Ω cm respectively for aluminium induced crystallized layers on glass at 500 °C.

Table 1: Hall hole concentration, resistivity and mobility of microcrystalline silicon from annealed glass/Al/a-Si at various annealing temperatures

Sample Number	Annealing Temp. (TA)/ °C	Hole concentration 1018 (cm-3)	Resistivity (Ω cm) 10-2	Mobility (cm2V-1s-1)
2112	470	9.2	3.9	17.3
219	520	4.7	7.4	17.9
2110B	520*	5.4	5.1	22.8

The values of hole densities are comparable with our results (in order of 1018) but our mobility values were comparable to their lower mobility range values of about 20 cm2 V-1s-1. High mobilities of 80 cm2V-1s-1 of polycrystalline silicon films prepared by thickening aluminium induced crystallization seed layers on wafer substrates using atmospheric pressure chemical vapour deposition have been obtained (Ishikawa, 2004)

4.0 Conclusion

Raman studies of the crystallized silicon films indicated that the crystallized films were predominantly of large crystallites. This was shown by the sharp crystalline Raman peaks which were centred at about 520 cm-1. The three-layer sample crystallization resulted in crystallization of the films at lower temperatures compared to the two-layer sample crystallizations. The onset of crystallization at low temperatures for the three-layer samples implies a reduction of the costs of production through shorter processing times and use of less energy at low annealing temperatures. The measured charge densities decreased with increase in annealing temperature and were in the order of 1018 cm-3. Mobilities of the films annealed at 470 °C and 520 °C were between 17-22.8 cm2 V-1s-1. These microcrystalline silicon seed layers could therefore be used for further deposition using other deposition methods such as hot wire chemical vapour deposition (HWCVD) or ion assisted deposition (IAD) for photovoltaic applications.

Acknowledgments

We would like to thank the German Exchange Service (DAAD) for funding the research visit at the Institute of Photovoltaics (IEF-5)-Forschungzentrum Juelich, Germany. The authors also acknowledge the assistance by Dr Aad Gordijn and Dr Thilo Kilper for some discussions on this work and Markus Huelsbeck for the Raman measurements. Many thanks also go to Uwe Rau and the management team at the institute for allowing the use of their equipment and for provision of materials for the project.

References

Avrami M. (1939), Transformation-time relations for random distribution of nuclei, *J. Chem. Phys.* **8**, pp. 212-224

Chandan B., Ghosh S.N., Solanki C. S. (2006). Aluminium induced crystallization of hot wire CVD deposited amorphous silicon, *Advances in energy research,* pp. 491-495.

Dimova-Malinovska D. (2005). Metal-induced crystallization – an advanced technology for producing polycrystalline silicon films on foreign substrates, in A

Vaseashta, D. Dimova-Malinovska, J.M. Marshall (eds), Nanostructured and advanced materials: Nato science series II: Mathematics, Physics and Chemistry, **204**, pp 31-50

Gall S., Lee K.Y., Dogan P., Gorka B., Becker C., Fenske F., Rau B., Conrad E., Rech B. (2007). Large-grained polycrystalline silicon thin-film solar cells on glass. 22nd European Photovoltaic Solar Energy Conference, Milan, Italy, pp. 2005-2009

Gordijn A., Rath J.K and Schropp R. E. I.(2006). High efficiency microcrystalline silicon solar cells made by very high frequency plasma enhanced chemical vapour deposition, *Prog. Photovolt. Res. Appl.* ***14,*** pp 305-311.

Gupta S., Chelewat H., Kumbhar, A.A., Adhikari S., Dusane R.O. (2008). Aluminum-induced in situ crystallization of HWCVD a-Si:H films, *Thin solid films 516,* pp850-852.

He D., Wang J. Y., Mittemeijer E.J. (2005). The initial stage of the reaction between amorphous silicon and crystalline aluminum, *Appl. Phys.* ***97,*** pp 093524- 093529

Hong W. E,. and Ro J. S. (2007). Millisecond crystallization of amorphous silicon films by Joule-heating induced crystallization using a conductive layer, *Thin solid films ,***515***,* pp. 5357-5361.

Hyeongnam K., Gyuyu L., Daewon K., Soo-Hong L. (2002). A study of polycrystalline silicon thin films as a seed layer in liquid phase epitaxy using aluminum-induced crystallization, *Current Applied Physics* **2***,* pp. 129-133.

Ishikawa Y., Nakamura A., Uraoka A., Fuyuki T. (2004). Polycrystalline silicon thin film for solar cells utilizing aluminum induced crystallization method, *Jpn J. Appl. Phys.,* 43(3), pp. 877-881.

Jaeger C., Antesberger T., Stutzmann M. (2008). Hydrogen passivation of ultra-thin low-temperature polycrystalline silicon films for electronic applications, *J. Non-cryst. Solids,* **324**, pp 2314-2318

Kondo M., Susuki S., Nasuno Y., Tanda M., Matsuda A. (2003) Recent developments in the high growth rate technique of device-grade microcrystalline silicon thin film, *Plasma Sources Sci. and Technol.* ***12***, pp S111-S116

Lee K.Y. , Becker C., Muske M., Ruske F., Gall S., Rech B., Bergniski M., Hüpkes J. (2007). Temperature stability of ZnO:Al film properties for poly-Si thin-film devices, *Appl. Phys. Lett.,* **91**, pp. 241911.

Lee K.Y., Becker C., Muske M., Gall S., Rech B. (2007). Poly-Si films grown on ZnO:Al coated glass by aluminum-induced layer exchange process. 22nd European Photovoltaic Solar Energy Conference, Milan, Italy, pp. 2028-2031.

Mahan A. H (2003). Hot wire chemical vapor deposition of Si containing materials for solar cells, *Solar Energy Materials and Solar Cells 78,* pp 299-327.

Nast O., Hartmann A. J. (2000). Influence of interface and Al structure on layer exchange during aluminium induced crystallization of amorphous silicon. J. Appl. Phys. **88 (2)**, pp 716-724

Nast O., Puzzer T., Koschier L. M., Sproul A.B., Wenham S.R. (1998). Aluminum-induced crystallization of amorphous silicon on glass substrates above and below the eutectic temperature, *Appl. Phys. Lett.,* **73(22)***,* pp. 3214-3216.

Pelant I., Fojtík P., Luterova K., Kocka J., Poruba A., Stepánek J. (2002). Electric-field-enhanced metal-induced crystallization of hydrogenated amorphous silicon at room temperature. *Appl. Phys. A,* **74**, pp. 557–560.

Rojas-López M., Orduña-Díaz A., Delgado-Macuil R., Olvera-Hernández J., Navarro-Contreras H., Vidal M. A., Saucedo N., Mendez-García V. H. (2007). AFM and FTIR characterization of microcrystalline Si obtained from isothermal annealing of Al/a-Si:H. *Phys. Status Solidi (a), 204(4), pp 1014–1017*

Schneider J., Schneider A., Sarikov A. , Klein J., Muske M., Gall S., Fuhs W. (2006). Aluminum-induced crystallization: Nucleation and growth process, *J. Non-Cryst. Solids 352, pp 972-975*

Wang C. L., Fan D.W., Sun S., Zhang F. J., Liu H. Z. (2009). Low-Temperature (< 100 °C), Poly-Si Thin Film Fabrication on Glass, *Chinese Physics Letters* **26(1)***,* pp 0181021

Wang J.Y., He D., Zhao Y.H., Mittemeijer E. J. (2006). Wetting and crystallization at grain boundaries: Origin of aluminum-induced crystallization of amorphous silicon, *Appl. Phys. Lett.* 88*,* pp. 061910.

Wang Z.M., Wang J.Y, Jeurgens L. P.H, Mittemeijer E. J. (2008a). Thermodynamics and mechanism of metal-induced crystallization in immiscible alloy systems: Experiments and calculations on Al/a-Ge and Al/a-Si bilayers. *Phys. Rev. B,* **77**, pp 045424

Wang Z.M., Wang J.Y, Jeurgens., P.H. L., Mittemeijer E. J. (2008b). Tailoring the ultrathin Al-induced crystallization temperature of amorphous silicon by application of interface thermodynamics, *Phys. Rev. Lett.* 100, pp. 125503.

Yamamoto K. (2003). Thin-film crystalline silicon solar cells, *Japan Soc. of Appl. Phys. International* (7), pp12-19.